The Tissue Factor Region That Interacts with Substrates Factor IX and Factor X

Daniel Kirchhofer,* Michael T. Lipari, Paul Moran, Charles Eigenbrot, and Robert F. Kelley

Departments of Cardiovascular Research and Protein Engineering, Genentech, Inc., 1 DNA Way, South San Francisco, California 94080

Received January 31, 2000; Revised Manuscript Received March 28, 2000

ABSTRACT: The enzymatic activity of coagulation factor VIIa is controlled by its cellular cofactor tissue factor (TF). TF binds factor VIIa with high affinity and, in addition, participates in substrate interaction through its C-terminal fibronectin type III domain. We analyzed surface-exposed residues in the C-terminal TF domain to more fully determine the area on TF important for substrate activation. Soluble TF (sTF) mutants were expressed in *E. coli*, and their ability to support factor VIIa-dependent substrate activation was measured in the presence of phospholipid vesicles or SW-13 cell membranes. The results showed that factor IX and factor X interacted with the same TF region located proximal to the putative phospholipid surface. According to the degree of activity loss of the sTF mutants, this TF region can be divided into a main region (residues Tyr157, Lys159, Ser163, Gly164, Lys165, Lys166, Tyr185) forming a solvent-exposed patch of 488 Å^2 and an extended region which comprises an additional 7−8 residues, including the distally positioned Asn199, Arg200, and Asp204. Some of the identified TF residues, such as Trp158 and those within the loop Lys159−Lys165, are near the factor VIIa γ-carboxyglutamic acid (Gla) domain, suggesting that the factor VIIa Gla-domain may also participate in substrate interaction. Moreover, the surface identified as important for substrate interaction carries a net positive charge, suggesting that charge interactions may significantly contribute to TF−substrate binding. The calculated surface-exposed area of this substrate interaction region is about 1100 Å^2, which is approximately half the size of the TF area that is in contact with factor VIIa. Therefore, a substantial portion of the TF surface (3000 Å^2) is engaged in protein−protein interactions during substrate catalysis.

The tissue factor (TF)[1]·factor VIIa (VIIa) complex initiates blood coagulation by proteolytic activation of substrate factors IX (IX) (*1*), X (X) (*2*), and VII (VII) (*3*). TF is composed of two fibronectin type III β-sandwich domains and serves as a cellular cofactor for VIIa, a serine protease with domain structures similar to other coagulation factors, such as IX, X, and protein C. Recent progress in our understanding of the interaction of TF with VIIa and with substrates indicates that the cofactor function of TF involves distinct surface-exposed regions in the N- as well as in the C-terminal TF domain. First, the TF contact region for VIIa runs from the membrane-proximal part of the C-terminal TF domain to the top of the N-terminal domain (*4*). The main portion of this 'binding strip' interacts with the VIIa light chain, and only the N-terminal TF domain makes contact with the catalytic domain of VIIa. The binding to VIIa does not induce any significant conformational changes on the TF molecule (*4*−*7*). In contrast, binding to TF reduces the domain flexibility of VIIa (*8*) and leads to conformational changes around and/or in the active site as suggested by the enhanced VIIa catalytic activity toward small synthetic substrates (*9*−*12*).

A different region of the TF molecule plays a role in macromolecular substrate recognition. The recognition of the substrate X involves TF residues Lys165 and Lys166 located in the C-terminal TF domain (*13*, *14*). These two residues are proximal to the membrane surface and may interact with the γ-carboxyglutamic acid domain (Gla) of X (*15*, *16*). Furthermore, it was suggested that the VIIa Gla may also contribute directly or indirectly to the TF-dependent interaction with X (*15*−*17*). In addition to Lys165 and Lys166, there seem to be additional residues in this TF area that may contribute to interaction with substrate X (*18*, *19*). However, their spatial relationship on the TF surface and the extent of the X interaction region on TF remained unclear. IX is another important substrate for the TF·VIIa complex (*1*). Activated IX in complex with its cofactor VIIIa converts X into Xa, and, therefore, TF·VIIa-mediated IX activation represents a very effective way to amplify reactions that lead to hemostasis, as demonstrated by use of in vitro flow systems (*20*). This view is consistent with the TF pathway-dependent activation of F·IX in vivo (*21*, *22*) and the severe bleeding diathesis associated with congenital IX deficiency (hemophilia B). Three studies, two of which used the TF mutant K165A:K166A (*15*, *23*) and another using the TF8-5G9 antibody (*24*), suggested that like X, IX may also interact with TF residues Lys165 and Lys166. However, it was not known whether additional TF residues were involved

* To whom correspondence should be addressed at the Department of Cardiovascular Research, ms#42, Genentech, Inc., 1 DNA Way, South San Francisco, CA 94080. Phone: (650) 225-2134. Fax: (650) 225-6327. E-mail: dak@gene.com.

[1] Abbreviations: TF, tissue factor; VII/VIIa, factor VII/VIIa; sTF, soluble tissue factor (1−219); IX/IXa, factor IX/IXa; X/Xa, factor X/Xa; PCPS phosphatidylcholine/phosphatidylserine; Gla, γ-carboxyglutamic acid; EGF, epidermal growth factor; HBSA, 20 mM Hepes (pH 7.5), 0.5 mg/mL BSA, 150 mM NaCl, and 5 mM $CaCl_2$.

10.1021/bi000182+ CCC: $19.00
Published on Web 05/27/2000

in IX recognition and, if so, how such an extended interaction site would be related to the X interaction site on TF. In fact, there are indications that different substrates may interact somewhat differently with the TF·VIIa complex (*19*, *23*).

To identify the full extent of the TF regions that interact with macromolecular substrates IX and X, we selected surface-exposed residues in the C-terminal TF domain and generated a panel of soluble TF (sTF) mutants. Functional analysis with different types of phospholipid surfaces demonstrated that both substrates interact with the same surface-exposed region located in the C-terminal TF domain. We will discuss different aspects of this region, such as its extent, contact sites on substrates, and function in ternary complex formation.

MATERIALS AND METHODS

Reagents. Fatty acid-free BSA was from Calbiochem (La Jolla, CA). Human recombinant VIIa was a gift from Mark O'Connell (Genentech, Inc.). X and IX were from Haematologic Technologies Inc. (Essex Junction, VT). Chromozym t-PA was from Boehringer Mannheim (Indianapolis, IN); Xa chromogenic substrate S2765 was from Diapharma Group Inc. (Columbus, OH) and IXa chromogenic substrate #299 from American Diagnostica (Greenwich, CT). Dioleoyl-1,2-diacyl-*sn*-glycero-3-(phospho-L-serine) (PS) and oleoyl-1,2-diacyl-*sn*-glycero-3-phosphocholine (PC) were from Avanti Polar Lipids Inc. (Alabaster, AL).

Site-Directed Mutagenesis, Expression, and Purification of sTF Mutants. Expression of sTF mutants (TF_{1-219}) in *E. coli* and subsequent purification on a D3 antibody affinity column were carried out as described earlier (*25*). For sTF mutants which did not bind to the D3 antibody column (N199A:R200A and K201A:D204A), a 7G11 antibody column was used. This column was prepared by coupling the 7G11 antibody to CNBr-activated Sepharose 4B (Pharmacia, Piscataway, NJ) according to the manufacturer's instructions. Cell pellets were stored at −20 °C for at least 1 h. The osmotic shock supernatants were applied to the antibody affinity column which was equilibrated with 50 mM Tris-HCl, pH 8.0, 500 mM NaCl (=buffer A). To remove nonspecifically bound proteins, the column was washed with 6 column volumes of buffer A and 50 mM Tris-HCl, pH 8.0, 1.0 M NaCl, 0.5 M tetramethylammonium chloride. sTF mutants were eluted with 0.1 M sodium acetate, pH 3.0, 0.2 M NaCl. Fractions were neutralized and peak fractions concentrated using a Centriprep 10 (Amicon, Beverly, MA). Protein concentrations were determined by absorbance measurements using an ϵ_{280} of 29.4 mM^{-1} cm^{-1} calculated from quantitative amino acid analysis data. An ϵ_{280} of 24 mM^{-1} cm^{-1} was used for the W158F mutant.

Amidolytic Activity of Soluble TF·VIIa Complex. Increasing concentrations of sTF mutants were incubated with VIIa in 20 mM Hepes, pH 7.5, containing 150 mM NaCl, 0.5 mg/mL BSA, and 5 mM $CaCl_2$ (HBSA buffer). After 20 min incubation, Chromozym t-PA was added, and the rates of amidolytic activity were measured at 405 nm on a kinetic microplate reader (Molecular Devices, Menlo Park, CA). The final concentrations of the reactants were as follows: 0.5−512 nM sTF mutants, 10 nM VIIa, 0.5 mM Chromozym t-PA. The background activity was defined as the amidolytic activity of VIIa in the absence of sTF mutants and was subtracted from the obtained values. The sTF concentrations that gave 50% VIIa saturation and the maximal rates of substrate cleavage were calculated by nonlinear curve fitting using Kaleidagraph 3.0.8 (Synergy Software, Reading, PA).

Preparation of Membrane Fractions of SW-13 Cells and TF-Expressing 293 Cells. SW-13 cells (primary small cell carcinoma; ATCC #CCL-105) were cultured in serum-supplemented medium. Production of human 293 kidney cells expressing recombinant TF_{1-263} was described (*26*). SW-13 and 293 cells were expanded in 850 cm^2 roller bottles (Corning Inc., Corning, NY) until they reached confluence. The cell layers were washed in PBS, detached with 10 mM EDTA, and centrifuged twice (2500 rpm on a Beckman GSA) for 5 min, with a PBS wash after the first centrifugation run. The cell pellet [$(4-5) \times 10^7$ cells/mL] was resuspended in 50 mM Tris, pH 7.5, and homogenized using a Dounce homogenizer, followed by centrifugation (2500 rpm) for 5 min at 4 °C. The membrane-containing supernatant fraction was collected and centrifuged at 45000*g* (Sorvall RC 5B, DuPont Co., Newtown, CT). The protein concentration of the cell membrane fraction was determined using the BCA assay (Pierce, Rockford, IL), and the membranes were stored in aliquots at −80 °C until use.

Factor X Activation Assay with Phospholipids and SW-13 Membranes. Phospholipid vesicles were prepared essentially as described (*27*) using dioleoyl-1,2-diacyl-*sn*-glycero-3-(phospho-L-serine) (PS) and oleoyl-1,2-diacyl-*sn*-glycero-3-phosphocholine (PC) (7:3 molar ratio). The PCPS vesicles together with VIIa and different concentrations of sTF mutants were incubated for 20 min in HBSA buffer. The reaction was started by adding X. The concentrations of reactants in this mixture were 0.1 nM VIIa, 0.5 mM PCPS, 200 nM X, and 200 nM sTF mutant. The same protocol was used for experiments with SW-13 cell membranes except that the reactant concentrations in the mixture were different: 0.6 nM VIIa, 300 μg/mL SW-13 cell membranes (total protein concentration), 200 nM X, and 200 nM sTF mutant. Fifty microliter aliquots of the reaction mixture were taken at different time points up to 2 min and quenched in 150 μL of 20 mM EDTA. In the second stage of the assay, 50 μL of 1.5 mM S2765 was added and the increase in absorption at 405 nm measured on a kinetic microplate reader (Molecular Devices). The linear rates of Xa generation were calculated and expressed as the relative activity (v_{mut}/v_{wt}) with respect to the activity of wild-type sTF (wt), which was included for each series of sTF mutants tested.

Factor IX Activation Assay with Phospholipids and SW-13 Membranes. PCPS vesicles together with VIIa and different concentrations of sTF mutants in HBSA buffer were incubated for 20 min, and the reaction was started by adding IX. The concentrations of reactants in this mixture were 0.6 nM VIIa, 0.5 mM PCPS, 400 nM IX, and 200 nM sTF mutant. The same protocol was used for experiments with SW-13 cell membranes except that the reactant concentrations in the mixture were different: 2.4 nM VIIa, 300 μg/mL SW-13 cell membranes (total protein concentration), 400 nM IX, and 200 nM sTF mutant. One hundred microliter aliquots of the reaction mixture were taken at different time points up to 2 min and quenched in 125 μL of 30 mM EDTA solution containing 60% ethylene glycol. Ethylene glycol enhances the amidolytic activity of IXa (*28*, *29*), and this property was utilized to measure IXa concentrations in the

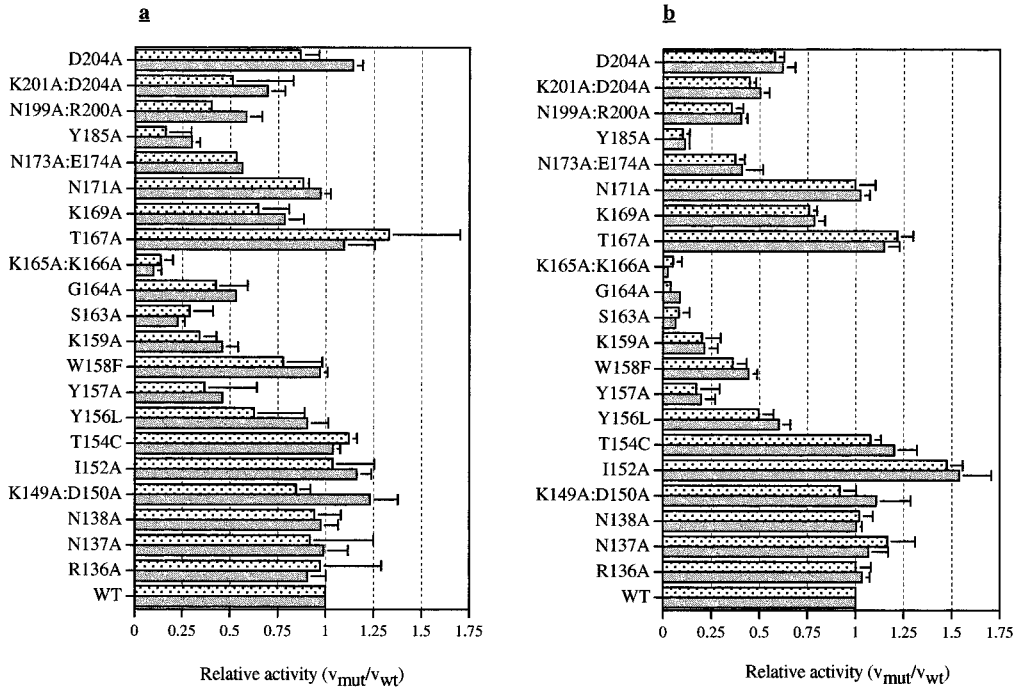

FIGURE 1: Effects of sTF mutants on VII-dependent activation of X and IX. Substrate activation rates were determined by adding a preformed complex of VIIa and sTF mutants (200 nM) to (a) 400 nM IX or (b) 200 nM X in the presence of either membrane fractions of SW-13 cells (dotted bars) or PCPS vesicles (gray bars). At time intervals, aliquots were removed from the reaction mixture and quenched and the concentrations of activated substrate measured with appropriate chromogenic substrates. The effects of sTF mutants were expressed as relative activities (v_{mut}/v_{wt}). The values are the mean ± SD of at least 3 independent experiments.

second stage of the assay as described recently (*30*). In the second stage of the assay, 25 μL of 5 mM chromogenic substrate #299 was added, and the increase in absorption at 405 nm was measured on a kinetic microplate reader (Molecular Devices). The linear rates of IXa generation were calculated and expressed as relative activity (v_{mut}/v_{wt}).

In some experiments, the activity of sTF mutants was measured over a wide range of sTF concentrations (0.25−256 nM). The maximal rates of IX and of X activation at saturating sTF mutant concentration and the 50% saturation of VIIa were calculated by nonlinear curve fitting using Kaleidagraph 3.0.8 (Synergy Software).

Inhibition of Tissue Factor Activity by 5G6 Antibody. The monoclonal anti-TF antibody 5G6 (Kirchhofer et al., submitted) or an isotype-matched control antibody (directed against nerve growth factor receptor) was incubated with cell membrane fractions of 293 cells expressing full-length TF_{1-263} and VIIa in HBSA for 20 min, after which X was added. The concentrations in this reaction mixture were as follows: 75 μg/mL TF_{1-263} membranes (total protein concentration), 0.04 nM VIIa, and 200 nM X. The same protocol was used for IX activation experiments except that the concentrations of VIIa and IX were 1 and 400 nM, respectively. At different time points, aliquots were removed, quenched in EDTA, and processed as described for the X and IX activation assays (see above).

Calculation of Solvent-Accessible Surface Area. Solvent-accessible surface area calculations were performed with the program XSAE of C. Broger (F. Hoffmann−La Roche, Basel, Switzerland) with a probe radius of 1.4 Å.

RESULTS

Effects of sTF Mutants on Activation of Substrates IX and X. Using the crystal structure of the TF·VIIa complex (*4*), we selected surface-exposed residues in the C-terminal TF domain for mutagenesis experiments. The sTF mutants were purified by affinity chromatography with anti-TF antibody columns, and their cofactor activity toward activation of IX and X was measured in enzyme assays. First, we employed a physiological phospholipid surface, such as membrane fractions derived from SW-13 cells to determine the function of sTF mutants. These cells do not express TF as indicated by clotting assays (data not shown) and substrate activation assays. At the employed saturating concentration (200 nM) of sTF mutants, the initial rates of substrate activation were 3.8 ± 0.8 nM IXa (nM VIIa)$^{-1}$ min^{-1} (n = 11) and 6.8 ± 2.7 nM Xa (nM F·VIIa)$^{-1}$ min^{-1} (n = 9), respectively. The activities of sTF mutants were expressed as ratios of initial rates of substrate activation by sTF mutant vs wild-type sTF (v_{mut}/v_{wt}). The results (Figure 1a) showed that the three sTF mutants S163A, K165A:K166A, and Y185A had less than 30% of wild-type activity for IX activation and the eight sTF mutants (Y156L, Y157A, K159A, G164A, K169A, N173A:E174A, N199A:R200A, K201A:D204A) had activities 30−75% of wild-type sTF. The other tested sTF mutants had activities similar to wild-type sTF (>75% of wild-type activity). Furthermore, all of the identified sTF mutants with reduced activity (<75% of wild-type sTF) toward IX also had reduced activity toward X (Figure 1b). In fact, most of these mutants showed slightly less activity for X than for IX activation, with the W158F and G164A mutants being substantially less active for X than for IX. This is consistent with results published by Huang et al. (*15*), showing that the TF mutant K165A:K166A retained more activity for IX activation than for X.

Since artificial phospholipid vesicles are commonly used to measure TF activity, we employed PCPS vesicles as an alternative phospholipid surface. When used at sufficiently

Table 1: Determination of sTF Mutant Concentrations That Gave 50% of Maximal VIIa Activity toward Activation of Macromolecular and Synthetic Substrates

sTF mutant	substrate = IX, ratio sTF_{mut}/sTF_{wt}[a]	substrate = X, ratio sTF_{mut}/sTF_{wt}[a]	substrate = Chromozym t-PA, ratio sTF_{mut}/sTF_{wt}[a]
R136A	1.5	0.7	0.8
N137A	0.6	0.8	0.3
N138A	1.4	0.9	1.0
K149A:D150A	2.4	1.1	11.4[b]
I152A	2.1	1.1	1.9
T154C	0.7	0.5	1.0
Y156L	0.8	0.3	3.3
Y157A	1.0	0.4	0.9
W158F	0.8	0.5	1.0
K159A	1.0	0.6	1.1
S163A	2.4	0.9	1.2
G164A	1.8	2.2	1.6
K165A:K166A	1.0	0.6	0.9
T167A	1.8	0.7	1.5
K169A	4.4	0.6	23.9[b]
N171A	0.6	0.2	0.4
N173A:E174A	14.1[b]	3.4	27.7[b]
Y185A	0.4	0.5	1.1
N199A:R200A	4.8	2.6	1.7
K201A:D204A	0.5	0.5	1.0
D204A	1.3	0.3	2.7

[a] Ratio of sTF concentrations (sTF_{mut}/sTF_{wt}) that gave 50% of maximal substrate activation rates. [b] sTF_{mut}/sTF_{wt} > 5-fold. The values for sTF mutants are the average of 2−3 experiments.

high concentrations, PCPS vesicles are very effective in supporting sTF·VIIa enzymatic activity toward macromolecular substrate (*31*, *32*). Using 0.5 mM PCPS, the rates of substrate activation by 200 nM wild-type sTF were 25.7 ± 6.8 nM IXa (nM VIIa)$^{-1}$ min^{-1} (n = 7) and 80.4 ± 35 Xa (nM VIIa)$^{-1}$ min^{-1} (n = 14), respectively. The results obtained with the sTF mutants under these conditions were largely identical to the results obtained with SW-13 cell membranes (Figure 1a,b). Therefore, despite the very different phospholipid environments and despite the fact that the rates of substrate conversion with SW-13 membranes was lower than with PCPS vesicles, the relative activities of the examined sTF mutants remained the same.

Binding of sTF Mutants to VIIa and Enhancement of F·VIIa Amidolytic Activity toward Small Synthetic Substrate. To exclude the possibility that reduced activities of sTF mutants were due to impaired interaction with VIIa, we carried out two different sets of experiments. First, we determined the sTF mutant concentrations that produced 50% of maximal VIIa activity toward IX and X. The results are summarized in Table 1 and demonstrated that the 50% VIIa saturation values for all sTF mutants were similar to wild type, consistent with BIAcore results (*25*), except for the mutant N173A:E174A. We interpret these data as indicating that sTF mutants maintained wild-type sTF binding to VIIa. This is consistent with the sTF mutants' normal binding to two monoclonal anti-TF antibodies, which recognize two nonoverlapping epitopes in the TF N-terminal domain (Kirchhofer et al., submitted for publication). Second, we examined the abilities of sTF mutants to enhance VIIa enzymatic function toward the small synthetic substrate Chromozym t-PA. As exemplified by the two sTF mutants K159A and S163A (Figure 2a), most of the mutants gave 50% enzyme saturation and maximal velocities similar to wild-type sTF (Table 1), despite reduced activities toward

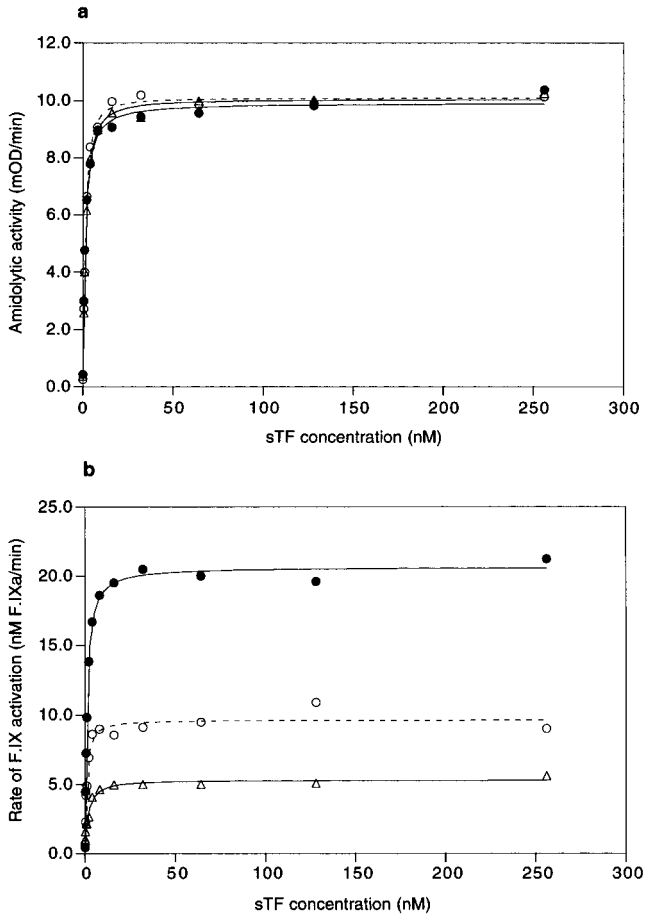

FIGURE 2: Activity of sTF mutants K159A and S163A on the VIIa-dependent activation of Chromozym t-PA and of IX. (a) Increasing concentrations of K159A (open circles), S163A (triangles), and wild-type sTF (filled circles) were incubated for 20 min with VIIa (10 nM) in 20 mM Hepes, pH 7.5, containing 0.5 mg/mL BSA, 150 mM NaCl, and 5 mM $CaCl_2$ (HBSA buffer). Chromozym t-PA (0.5 mM) was added and the rate of substrate cleavage (mOD/min) monitored at 405 nm. (b) sTF mutants or sTF wild type were incubated for 20 min with VIIa (0.6 nM) and PCPS vesicles (0.5 mM) in HBSA buffer. IX (400 nM) was added, timed aliquots were quenched, and activated IX was quantified in the second stage of the assay using a chromogenic substrate. Results are expressed as the initial rates of IXa formation (nM IXa min^{-1}) as a dependence of sTF concentration. The values are the average of two independent experiments.

macromolecular substrate (Figure 2b). These results indicated that the sTF cofactor function with respect to VIIa binding and enhancement of VIIa active site activity were not disturbed. The only exceptions were sTF mutants K149A:D150A, K169A, and N173A:E174A, which gave significantly increased values in the Chromozym t-PA assay (Table 1). In an earlier study, these three mutants showed wild-type K_D values for VIIa binding (*25*). Therefore, the reason for the differences observed in the amidolytic assay remains unclear.

Effects of sTF Mutations on Kinetic Constants of X Activation. We determined the kinetic constants for X activation in the presence of 0.5 mM PCPS vesicles. Unfortunately, because of the very low specific activity of the IXa chromogenic substrate (#299), a similar kinetic analysis for IX activation was not feasible. For X as substrate, the K_M for sTF wild type was 387 nM, similar to a previously determined value using sTF (*32*). All four examined sTF mutants (Y157A, S163A, G164A, and Y185A) increased K_M

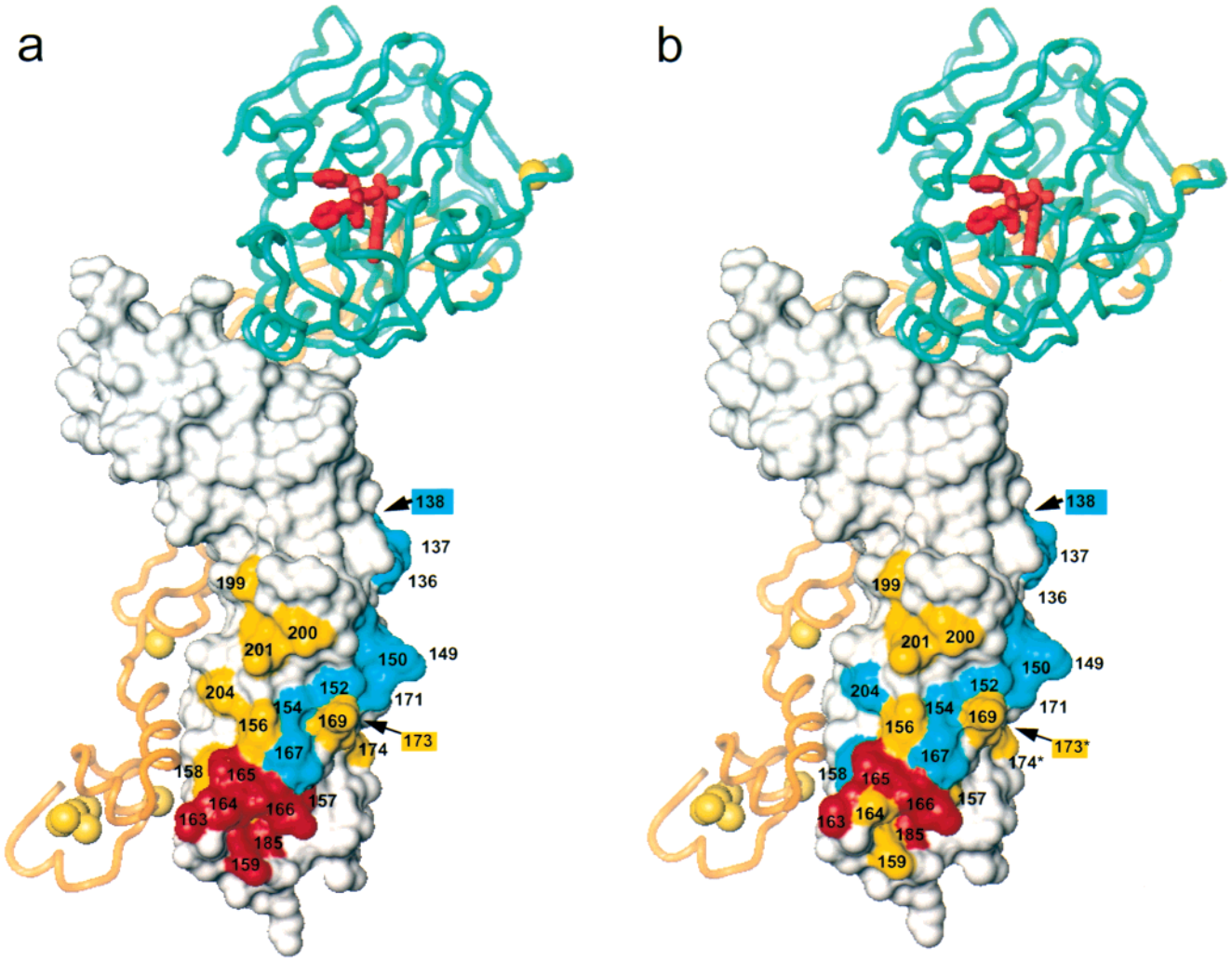

FIGURE 3: Localization of the X and IX substrate interaction region of TF in the crystal structure of the TF·VIIa complex (*4*). VIIa is colored with the light chain in orange and the heavy chain in green-blue. The active site inhibitor (D-Phe-L-Phe-Arg chloromethyl ketone) is in red, and the calcium atoms are in yellow. Tissue factor (gray) is in a solvent-accessible representation. Shown are the TF residues that, according to substrate activation assays performed in the presence of SW-13 cell membranes, gave relative activities (v_{mut}/v_{wt}) of <0.3 (red), 0.3−0.75 (yellow), and >0.75 (blue) for activation of (a) X and (b) IX. The asterisk (*) indicates the residues which upon mutation resulted in reduced binding affinity (sTF_{mut}/sTF_{wt} > 5) for VIIa in macromolecular substrate activation assays (see Table 1). The figures were produced using Insight II (MSI, San Diego, CA).

Table 2: Kinetic Constants for sTF·VIIa-Mediated Activation of X[a]

sTF	K_M ($\times 10^{-9}$ M)	k_{cat} (s^{-1})	k_{cat}/K_m ($\times 10^6$ M^{-1} s^{-1})
wild-type	387 ± 68	5.7 ± 0.5	14.7
Y157A	1323 ± 316	2.5 ± 0.4	1.9
S163A	2059 ± 829	1.9 ± 0.2	0.9
G164A	2543 ± 623	1.9 ± 0.2	0.8
Y185A	1766 ± 462	2.4 ± 0.4	1.4

[a] Enzyme assays were carried out at saturating sTF concentrations (100 nM) over a range of X concentrations (7.8−3000 nM) in the presence of 0.1 nM VIIa and 0.5 mM PCPS vesicles. K_M and k_{cat} values were calculated from initial X activation rates vs X concentration plots using the Michaelis−Menten equation. The values are the means of 3−5 experiments ± SD.

and reduced k_{cat} values (Table 2). The sTF mutant G164A displayed the strongest effects, increasing K_M by 6.5-fold and decreasing k_{cat} by 3-fold. The tested sTF mutants had second-order rate constants that were 8−18-fold reduced with respect to the sTF wild-type value (Table 2). These results are in agreement with the effects observed with the two full-length TF mutants K165A:K166A (*15*, *23*) and W158R:S160G (*23*), both of which affected K_M as well as k_{cat} values.

Location of the IX and X Interaction Region on the TF·F·VIIa Structure. TF residues that were found to play a role in the activation of macromolecular substrates are displayed on the structure of TF·VIIa (*4*) in Figure 3. The TF residues were divided into three groups according to their relative activities in the SW-13 cell membrane assays (<30% activity = red; 30−75% activity = yellow; >75% activity = blue). For the tested sTF double mutants, both residues were classified into the same group, even though differences in the importance of the individual residues may exist. Since the double mutant K201A:D204A, but not the single mutant D204A, had reduced activity in the IX assay, it was concluded that K201A was responsible for the observed effect. Furthermore, in the originally published structure (*4*), the surface loop Lys159−Ser162 was disordered. Therefore, we used the TF·5G9 structure (*33*), in which this loop is resolved, for this part of TF. As seen in Figure 3, the seven most important TF residues for activation of both substrates (Tyr157, Lys159, Ser163, Gly164, Lys165, Lys166, Tyr185) are located in proximity to the presumed membrane surface. They form a surface patch with a calculated area of 488 Å^2

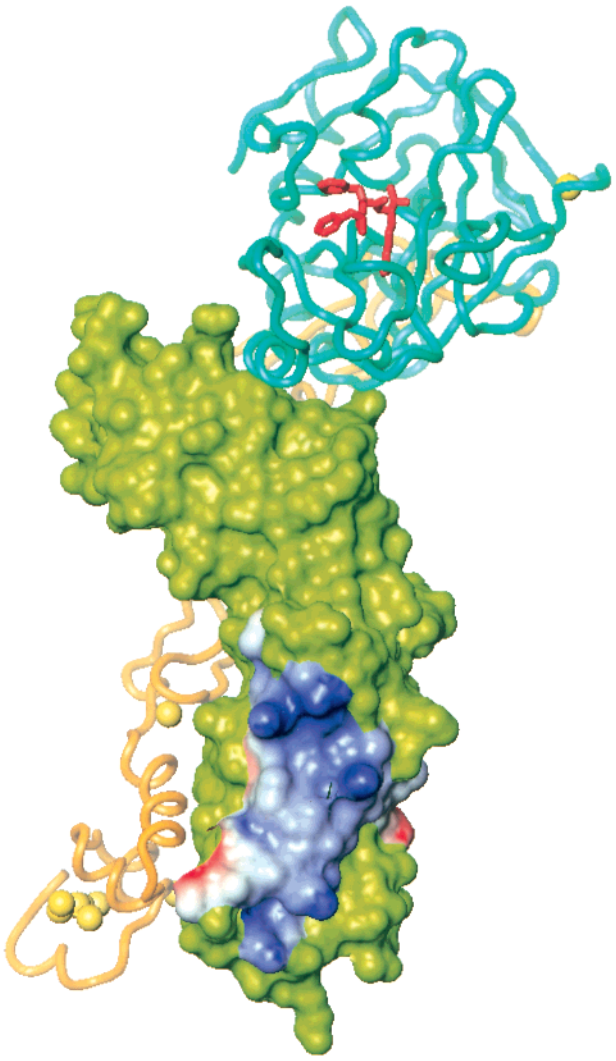

FIGURE 4: Electrostatic potential calculated for TF·VIIa is displayed on the solvent-exposed surface of the area of TF identified as important for substrate activation. The heavy and light chains of VIIa are shown as tubes colored green-blue and orange, respectively, and the VIIa active site is occupied by the inhibitor (red) from the X-ray structure of TF·VIIa (*4*). Calcium ions are yellow spheres. The TF surface is colored green, except for the interaction region, where blue indicates the net positive charge and red the net negative charge. The figure was prepared using InsightII (MSI, San Diego).

(red area for F·X), which we consider the main substrate interaction region. From this patch, the substrate interaction region runs to the top of the C-terminal TF domain. The extended X interaction region which includes the main interaction region (488 Å^2) and residues Tyr156, Lys169, Asn173, Glu174, Asn199, Arg200, Lys201, and Asp204 (for X only) comprise a surface-accessible area of 1144 Å^2. For IX, the respective value is 1074 Å^2, about 10% less than for X as substrate. For all calculations, the residue Trp158 was omitted since we assumed this residue to be buried within the VIIa contact site (*4*). Using the published TF·VIIa structure (*4*), we calculated that the surface in contact with VIIa is 1915 Å^2. Therefore, the extended TF substrate interaction region (1074−1144 Å^2) is about half the size of the VIIa interaction area.

Also, we calculated the net electrostatic potential for the TF·VIIa complex and found the interaction region has a net positive charge on the solvent-accessible surface (Figure 4). The main contributors to the positive charge are side chains

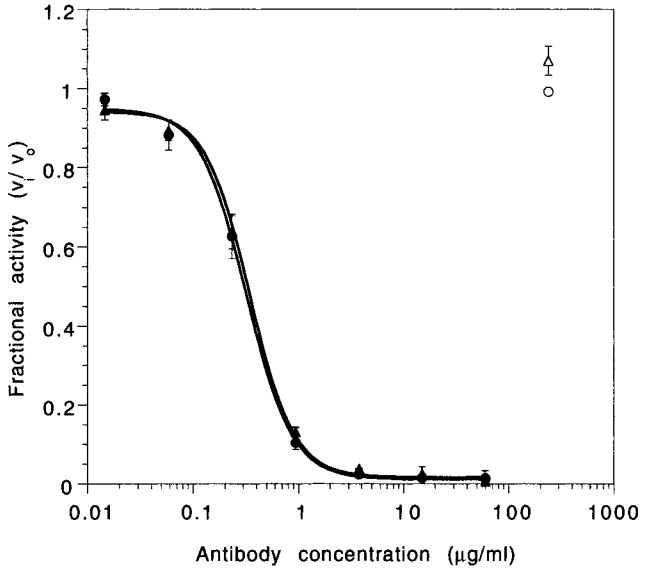

FIGURE 5: Inhibition of IX and X activation by anti-TF antibody 5G6. Membrane fractions of TF_{1-263} expressing 293 cells were incubated for 20 min with VIIa (0.1 nM) and monoclonal anti-TF antibody 5G6 or an isotype-matched irrelevant control antibody (control). IX (400 nM) or X (200 nM) was added to start the reaction, and aliquots were removed at different time points and processed as described under Materials and Methods. Inhibition was expressed as fractional activity of substrate conversion (v_i/v_o). The values are the mean ± SD of 3 independent experiments. IX, filled circles; X, filled triangles; control, open symbols.

of residues Lys159, Lys165, Lys166, and Lys169. The depiction of residues important for substrate turnover has used the TF·VIIa structure as a template. There are likely to be structural changes in this complex when substrate binds, but they are probably small. The calculation of electrostatic potential at the molecular surface is relatively sensitive to such changes, but the preponderance of lysine residues within the interaction zone, and the absence of compensating aspartate or glutamate residues, means a net positive potential would be retained.

Effects of Anti-TF Antibody 5G6 on IX and X Activation. The epitope of the anti-TF antibody 5G6 overlaps with the described IX and X interaction region of TF. It includes TF residues Ile152, Lys165, Lys166, Asn199, Arg200, and Lys201 (Kirchhofer et al., submitted for publication), and, therefore, 5G6 should interfere with the activation of both IX and X. In agreement with this prediction, we found that 5G6 inhibited activation of both substrates when either full-length TF_{1-263} (Figure 5) or sTF (data not shown) was used in the assays.

DISCUSSION

This study shows that two important substrates of the TF·VIIa enzymatic complex, IX and X, interact with a shared interaction site located on the C-terminal fibronectin type III domain of TF. In most cases, the sTF mutants used to map this region impaired the activation of X more severely than IX, similar to observations made by Huang et al. (*15*) with the TF mutant K165A:K166A. However, these differences were generally small and may simply reflect the better ability of IX to accommodate mutations in this interaction region. Nevertheless, the TF residues found to be important for X activation were largely identical to those for IX even

when different phospholipid surfaces, such as PCPS vesicles and SW-13 cell membranes, were used. In agreement with a shared TF interaction region, the activation of both IX and X was completely inhibited by an anti-TF antibody which binds to this TF region, similar to results obtained with the related anti-TF antibody TF8-5G9 (*24*, *33*, *34*). In the following, three different aspects of this shared substrate interaction region will be discussed, i.e., the extent of the region, possible interaction site(s) on substrates, and the role of this TF region in the ternary cofactor·enzyme·substrate complex.

First, the substrate interaction region can be divided into two parts: the main region which consisted of residues Tyr157, Lys159, Ser163, Gly164, Lys165, Lys166, and Tyr185 with a surface area of about 488 Å^2, and the extended region comprising an additional 7−8 residues which showed less dramatic effects on substrate activation. The total calculated surface area covered by the entire region was 1074−1144 Å^2, which is substantially larger than the calculated buried surface reported by Ruf (*16*) using computational docking of the X Gla-domain to TF·VIIa. With the caveat that the number of residues which actually contact substrate may be smaller or larger than identified by mutagenesis experiments, our results indicate that the TF area interacting with substrate is about half the size of the TF surface contacting enzyme VIIa. Therefore, a substantial portion of TF surface (about 3000 Å^2) is engaged in protein−protein interactions during substrate catalysis. Some residues within the main substrate interaction region were identified previously and included Lys165 and Lys166 (*13*−*15*) as well as residues within the TF sequence 157−167 that was investigated by Rehemtulla et al. (*18*) and Ruf et al. (*19*). The only noted discrepancy concerned the role of TF residue Lys159, which we find to be part of the main interaction region for both IX and X, whereas Ruf et al. (*19*) suggested a specific role of this residue for VII activation but not for activation of X. In our systems, the K159A sTF mutant gave strongly reduced activation rates for IX and X and with both examined types of phospholipid surfaces. It could be that the test system used by Ruf et al. (*19*) was generally less sensitive to detect TF dysfunction, as suggested by the observed moderate loss of activity by the double mutant K165A:K166A (*19*), whereas we and others found a >90% reduction of X activation rates (*13*, *15*).

Several TF residues found to be important for IX and X activation are located in the surface-exposed loop Lys159−Gly164 situated proximal to the VIIa Gla-domain. Particularly, residues Ser162 and Ser163 are sufficiently close for a possible interaction with the VIIa Gla-domain. The importance of the Lys159−Gly164 loop and Trp158 for substrate activation together with their potential interaction with the VII Gla-domain strongly suggested that the VIIa Gla-domain plays a role in the recognition of IX and X. This is consistent with conclusions made by others using Gla-domain less VIIa (*15*, *35*), VIIa-Gla mutants (*16*), and synthetic VII Gla-domain (*17*).

Second, electrostatic analysis of the substrate interaction region revealed a predominantly positive net charge. Therefore, it is reasonable to assume that charge interactions play a significant role in the molecular interaction between this TF region and substrate. In fact, Ruf et al. (*16*) suggested that negatively charged γ-carboxyglutamic acid and Asp residues within the X Gla-domain may be involved in such interactions. A role of X or the IX Gla-domain as the TF contact partner was suggested by others (*15*, *16*) and is consistent with the proximity of the identified TF substrate interaction region to the membrane surface. In agreement with this view, a naturally occurring IX Gla-domain mutant (G12R) showed reduced TF·VII-dependent activation despite normal phospholipid binding (*36*). Additional TF−substrate interactions may involve three TF residues (Asn199, Arg200, Lys201) located distally to the phospholipid surface. It is conceivable that they interact with substrates by binding to the C-terminal portion of the Gla-domain or the epidermal growth factor 1 (EGF1) domain. In support of this hypothesis, Zhong et al. (*37*) showed evidence for a role of the IX−EGF1 domain in the activation of IX by the TF·VIIa complex. However, a direct involvement of the three TF residues in a possible EGF1 contact remains to be shown.

Third, the substrate interaction domain of TF could serve to properly align IX and X to form a productive ternary TF·VIIa·substrate complex. In this respect, the TF−substrate interaction in combination with the phospholipid anchoring of substrate may significantly reduce rotational diffusion of substrate (*38*) and provide optimal orientation with respect to the TF·VIIa complex. This TF−substrate interaction is one of multiple protein−protein interactions between substrate and the TF·VIIa complex. Other interactions, besides a possible EGF1−TF interaction, include those between the substrate and VIIa catalytic domains, such as interactions with VIIa exosites (*39*) and with the VIIa catalytic cleft. The fact that the sTF mutants described here as well as two previously reported TF mutants, K165A:K166A (*15*, *23*) and W158R:S160G (*23*), affected the k_{cat} value implied that the substrate interaction region of TF has functions beyond solely providing binding energy. The possibility that the TF mutants may have affected k_{cat} due to long-range conformational changes on TF is unlikely, since VIIa amidolytic activity as well as binding to two different anti-TF antibodies was unchanged. We interpret the results to say that the substrate site interacting with this TF region, i.e., the Gla-domain, is functionally linked to the substrate site that contacts the VIIa catalytic domain. Thus, mutations that lead to perturbations in the TF−substrate Gla interaction may cause perturbations in the catalytic domain interactions and consequently affect k_{cat}. Another implication of a functional interdependence between these two sites is that an initial TF−substrate interaction could significantly increase the 'effective' substrate concentration for a subsequent interaction between scissile peptide and catalytic cleft. Therefore, even if the affinities of the two individual contact regions are low, the overall affinity could be increased dramatically as shown for bifunctional proteins (*40*, *41*). For instance, the bifunctional inhibitor consisting of a TF construct that is optimally linked to a Kunitz domain binds to VIIa with more than 100-fold increased affinity as compared to the single components (*41*). Therefore, it is conceivable that TF, via its substrate interaction region, establishes initial substrate contact, after which further substrate−VIIa interactions ensue, similar to a scheme proposed for the prothrombinase complex (*42*).

Since TF-dependent coagulation may also involve autoactivation of VII by TF·VIIa (*3*, *43*, *44*), the question arises whether substrate VII (alone or as TF·VII complex) would interact with the same TF region as do the substrates IX and

X. We have not examined this interaction experimentally, but our results with IX and X indicated that the identified TF region seems optimally suited to interact with Gla-domains of substrates and, thus, may also interact with the VII Gla-domain. Consistent with this assumption, an anti-TF antibody which binds to this substrate interaction region blocks VII activation by TF·VIIa (*24*). Another example for the importance of this TF region in interacting with Gla-containing protein partners is the Xa-dependent inhibition of TF·VIIa by tissue factor pathway inhibitor (*45*). Together, these results suggest a generalized function of this TF region in mediating interactions with Gla-containing interaction partners. Therefore, it may not be surprising that this substrate interaction region seems not involved in TF·VIIa enzymatic activity toward the cofactors VIII and V (*46*), both of which do not contain Gla-domains.

In conclusion, the results demonstrate the presence of a TF region which serves as an important interaction site for two substrates. This further highlights the complexity of TF-mediated protein interactions, the sum of which make up TF's cofactor function. It will be interesting to see whether the identified TF substrate interaction region or other TF surface areas outside the VIIa interface region participate in some recently discovered TF functions, such as TF-dependent cellular signal transduction.

REFERENCES

1. Østerud, B., and Rapaport, S. I. (1977) *Proc. Natl. Acad. Sci. U.S.A. 74*, 5260−5264.
2. Nemerson, Y. (1966) *Biochemistry 5*, 601−608.
3. Nakagaki, T., Foster, D. C., Berkner, K. L., and Kisiel, W. (1991) *Biochemistry 30*, 10819−10824.
4. Banner, D. W., D'Arcy, A., Chene, C., Winkler, F. K., Guha, A., Konigsberg, W. H., Nemerson, Y., and Kirchhofer, D. (1996) *Nature 380*, 41−46.
5. Muller, Y. A., Ultsch, M. H., Kelley, R. F., and de Vos, A. M. (1994) *Biochemistry 33*, 10864−10870.
6. Harlos, K., Martin, D. M. A., O'Brien, D. P., Jones, E. Y., Stuart, D. I., Polikarpov, I., Miller, A., Tuddenham, E. G. D., and Boys, C. W. G. (1994) *Nature 370*, 662−666.
7. Zhang, E., Charles, R. S., and Tulinsky, A. (1999) *J. Mol. Biol. 285*, 2089−2104.
8. Waxman, E., Laws, W. R., Laue, T. M., Nemerson, Y., and Ross, J. B. A. (1993) *Biochemistry 32*, 3005−3012.
9. Lawson, J. H., Butenas, S., and Mann, K. G. (1992) *J. Biol. Chem. 267*, 4834−4843.
10. Neuenschwander, P. F., Branam, D. E., and Morrissey, J. H. (1993) *Thromb. Haemostasis 70*, 970−977.
11. Butenas, S., Ribarik, N., and Mann, K. G. (1993) *Biochemistry 32*, 6531−6538.
12. Higashi, S., Nishimura, H., Fujii, S., Takada, K., and Iwanaga, S. (1992) *J. Biol. Chem. 267*, 17990−17996.
13. Roy, S., Hass, P. E., Bourell, J. H., Henzel, W. J., and Vehar, G. A. (1991) *J. Biol. Chem. 266*, 22063−22066.
14. Ruf, W., Miles, D. J., Rehemtulla, A., and Edgington, T. S. (1992) *J. Biol. Chem. 267*, 6375−6381.
15. Huang, Q., Neuenschwander, P. F., Rezaie, A. R., and Morrissey, J. H. (1996) *J. Biol. Chem. 271*, 21752−21757.
16. Ruf, W., Shobe, J., Rao, S. M., Dickinson, C. D., Olson, A., and Edgington, T. S. (1999) *Biochemistry 38*, 1957−1966.
17. Martin, D. M. A., O'Brien, D. P., Tuddenham, E. G. D., and Byfield, P. G. H. (1993) *Biochemistry 32*, 13949−13955.
18. Rehemtulla, A., Ruf, W., Miles, D. J., and Edgington, T. S. (1992) *Biochem. J. 282*, 737−740.
19. Ruf, W., Miles, D. J., Rehemtulla, A., and Edgington, T. S. (1992) *J. Biol. Chem. 267*, 22206−22210.
20. Repke, D., Gemmell, C. H., Guha, A., Turitto, V. T., Broze, G. J., Jr., and Nemerson, Y. (1990) *Proc. Natl. Acad. Sci. U.S.A. 87*, 7623−7627.
21. Bauer, K. A., Kass, B. L., ten Cate, H., Hawiger, J. J., and Rosenberg, R. D. (1990) *Blood 76*, 731−736.
22. Bauer, K. A. (1997) *Thromb. Haemostasis 78*, 108−111.
23. Dittmar, S., Ruf, W., and Edgington, T. S. (1997) *Biochem. J. 321*, 787−793.
24. Fiore, M. M., Neuenschwander, P. F., and Morrissey, J. H. (1992) *Blood 80*, 3127−3134.
25. Kelley, R. F., Costas, K. E., O'Connell, M. P., and Lazarus, R. A. (1995) *Biochemistry 34*, 10383−10392.
26. Paborsky, L. R., Tate, K. M., Harris, R. J., Yansura, D. G., Band, L., McCray, G., Gorman, C. M., O'Brien, D. P., Chang, J. Y., Swartz, J. R., Fung, V. P., Thomas, J. N., and Vehar, G. A. (1989) *Biochemistry 28*, 8072−8077.
27. Mimms, L. T., Zampighi, G., Nozaki, Y., Tanford, C., and Reynolds, J. A. (1981) *Biochemistry 20*, 833−840.
28. Neuenschwander, P. F., McCoullough, J., McCallum, C. D., and Johnson, A. E. (1997) *Thromb. Haemostasis 78* (*Suppl.*), 428.
29. Sturzebecher, J., Kopetzki, E., Bode, W., and Hopfner, K.-P. (1997) *FEBS Lett. 412*, 295−300.
30. Refino, C. J., Himber, J., Burcklen, L., Moran, P., Peek, M., Suggett, S., Devaux, B., and Kirchhofer, D. (1999) *Thromb. Haemostasis 82*, 1188−1195.
31. Fiore, M. M., Neuenschwander, P. F., and Morrissey, J. H. (1994) *J. Biol. Chem. 269*, 143−149.
32. Kelley, R. F., Refino, C. J., O'Connell, M. P., Modi, N., Sehl, P., Lowe, D., Pater, C., and Bunting, S. (1997) *Blood 89*, 3219−3227.
33. Huang, M., Syed, R., Stura, E. A., Stone, M. J., Stefanko, R. S., Ruf, W., Edgington, T. S., and Wilson, I. A. (1998) *J. Mol. Biol. 275*, 873−894.
34. Ruf, W., and Edgington, T. S. (1991) *Thromb. Haemostasis 66*, 529−533.
35. Ruf, W., Kalnik, M. W., Lund-Hansen, T., and Edgington, T. S. (1991) *J. Biol. Chem. 266*, 15719−15725.
36. Larson, P. J., Stanfield-Oakley, S. A., VanDusen, W. J., Kasper, C. K., Smith, K. J., Monroe, D. M., and High, K. A. (1996) *J. Biol. Chem. 271*, 3869−3876.
37. Zhong, D., Smith, K. J., Birktoft, J. J., and Bajaj, S. P. (1994) *Proc. Natl. Acad. Sci. U.S.A. 91*, 3574−3578.
38. Gentry, R., Ye, L., and Nemerson, Y. (1995) *Biophys. J. 69*, 362−371.
39. Dickinson, C. D., Kelly, C. R., and Ruf, W. (1996) *Proc. Natl. Acad. Sci. U.S.A. 93*, 14379−14384.
40. Jencks, W. P. (1981) *Proc. Natl. Acad. Sci. U.S.A. 78*, 4046−4050.
41. Lee, G. F., Lazarus, R. A., and Kelley, R. F. (1997) *Biochemistry 36*, 5607−5611.
42. Krishnaswamy, S., and Betz, A. (1997) *Biochemistry 36*, 12080−12086.
43. Yamamoto, M., Nakagaki, T., and Kisiel, W. (1992) *J. Biol. Chem. 267*, 19089−19094.
44. Neuenschwander, P. F., Fiore, M. M., and Morrissey, J. H. (1993) *J. Biol. Chem. 268*, 21489−21492.
45. Rao, L. V. M., and Ruf, W. (1995) *Biochemistry 34*, 10867−10871.
46. Neuenschwander, P. F., Safa, O., Huang, Q., and Morrissey, J. H. (1999) *Thromb. Haemostasis, Suppl.* (*Abstr.*), 465−466.

BI000182+